

Spectral Power Parameter Estimation of Random Sources with Binary Sampled Signals

Manuel S. Stein

Abstract—This paper investigates the problem of estimating the spectral power parameters of random analog sources using numerical measurements acquired with minimum digitization complexity. Therefore, spectral analysis has to be performed with binary samples of the analog sensor output. Under the assumption that the structure of the spectral power density of the analog sources is given, we investigate the achievable accuracy for power level estimation with likelihood-oriented processing. The discussion addresses the intractability of the likelihood with multivariate hard-limited samples by exploiting advances on probabilistic modeling and statistical processing of hard-limited multivariate Gaussian data. In addition to estimation-theoretic performance analysis, the results are verified by running an iterative likelihood-oriented algorithm with synthetic binary data for two exemplary sensing setups.

Index Terms—binary sensing, estimation, exponential family, maximum likelihood, spectral analysis, 1-bit ADC

I. INTRODUCTION

Analyzing hard-limited sensor data is a traditional topic in signal processing. Early approaches [1], [2] were motivated by the lack of computing power, which hindered the processing with high amplitude resolution [3], [4]. In recent work, amplitude resolution minimization has again received attention due to data transmission [5] or analog-to-digital (A/D) conversion constraints [6], [7], [8], [9], [10]. Combining both aspects indicates that signal digitization via binary sampling is also key for high-performance sensing systems. The simplicity of basic digital processing steps, small sensor data volume, and energy-efficient analog front-end design make it possible to deploy higher temporal, spectral, and spatial sampling rates. Such, with the same A/D resources, digital measurements can be acquired, which contain more information about the analog signal model [11]. To extract all this information from the data, efficient binary signal processing methods are required.

In this context, likelihood-oriented spectral analysis with noisy binary measurements is discussed. We assume that the analog signal is a superposition of ideally band-limited Gaussian processes, each characterized by a spectral power density of unknown weight. In practice, such an assumption is never exactly fulfilled. However, in several applications, signals approximately follow such additive random models [12]. Besides, within the class of distributions with the same covariance structure, the Gaussian one has maximum entropy [13]. This theoretical argument supports the practical relevance of the Gaussian assumption by suggesting that it forms a conservative modeling perspective. Here the analog signal is

digitized via a low-complexity binary sampling device while the digital sensor data shall be processed optimally. This requires characterization of the likelihood which is intractable for multivariate binary distributions. We address this by using a binary distribution model with reduced sufficient statistics which provides access to a conservative version of the Fisher information matrix [14]. Based on this framework, we investigate the sensitivity gap in comparison to sampling the analog signal with high A/D resolution and verify the results by Monte-Carlo simulations of an iterative estimation algorithm.

Note that, direct estimation of the spectrum function from hard-limited data is considered in [1], [2], [3] using an asymptotic relationship between quantized and unquantized autocorrelation. Approximate maximum-likelihood estimators (MLEs) for the parameters of an autoregressive process are derived in [15] by exploiting the asymptotic independence between distant samples of a Gaussian process. In contrast, here the estimation of spectral parameters characterizing the analog random process is considered under an auxiliary likelihood applicable also to samples of small size. For the distinct problem of estimating the parameters of deterministic sinusoidal signals in white noise from hard-limited samples, see e.g., [16].

II. SYSTEM MODEL

For the discussion, we assume an analog sensor signal

$$y(t) = \sum_{d=1}^D x_d(t) + \eta(t), \quad y(t) \in \mathbb{R}, t \in \mathbb{R}, \quad (1)$$

comprising $D \in \mathbb{N}$ source signals

$$x_d(t) = x_{c,d}(t) \cos(t\omega_d) + x_{s,d}(t) \sin(t\omega_d), \quad (2)$$

each with an individual frequency $\omega_d \in \mathbb{R}$. The components $x_{c/s,d}(t) \in \mathbb{R}$ are random processes with power spectral density $\Psi_d(\omega) = \theta_d, \theta_d > 0$, for $\omega \in [-\Omega_d; \Omega_d]$ and $\Psi_d(\omega) = 0$ elsewhere. The auto-correlation of such random processes is

$$\begin{aligned} r_d(t) &= \mathbb{E}_{x_{c/s}} [x_{c/s,d}(\tau)x_{c/s,d}(\tau - t)] \\ &= \frac{1}{2\pi} \int_{-\Omega_d}^{\Omega_d} \Psi_d(\omega) e^{j\omega t} d\omega \\ &= \theta_d \frac{\Omega_d}{\pi} \operatorname{sinc}\left(\frac{\Omega_d}{\pi} t\right). \end{aligned} \quad (3)$$

In (1), $\eta(t) \in \mathbb{R}$ denotes independent additive noise which is also modeled as an ideally band-limited random process with $\Psi_0(\omega) = \theta_0$ for $\omega \in [-\Omega_0; \Omega_0]$ and $\Psi_0(\omega) = 0$ elsewhere.

This work was funded by the Deutsche Forschungsgemeinschaft (DFG, German Research Foundation) - grant no. 413008418.

M. S. Stein is with the Department of Microelectronics, Technische Universiteit Delft, The Netherlands (e-mail: M.S.Stein@tudelft.nl).

A. Digital data model - Ideal sampling

Sampling (1) at a rate of $f_{A/D} = \frac{\Omega_{A/D}}{\pi}$ for a duration of $T_{A/D} = \frac{M}{f_{A/D}}$, $M \in \mathbb{N}$, with an A/D converter featuring ∞ -bit amplitude resolution, results in M -variate samples of the form

$$\mathbf{y} = \sum_{d=1}^D \mathbf{x}_d + \boldsymbol{\eta}, \quad \mathbf{y}, \mathbf{x}_d, \boldsymbol{\eta} \in \mathbb{R}^M, \quad (4)$$

with a covariance matrix of structure

$$\begin{aligned} \mathbf{R}_y(\boldsymbol{\theta}) &= \mathbb{E}_{\mathbf{y};\boldsymbol{\theta}} [\mathbf{y}\mathbf{y}^T] \\ &= \sum_{d=1}^D \theta_d \frac{\Omega_d}{\pi} \boldsymbol{\Sigma}_d \odot \mathbf{W}_d + \theta_0 \frac{\Omega_0}{\pi} \boldsymbol{\Sigma}_0, \end{aligned} \quad (5)$$

$$\boldsymbol{\theta} = [\theta_1 \quad \dots \quad \theta_D \quad \theta_0]^T. \quad (6)$$

The entries of the source and noise correlation matrices are

$$[\boldsymbol{\Sigma}_d]_{ij} = \text{sinc} \left(\frac{\Omega_d}{\Omega_{A/D}} |i - j| \right), \quad i, j = 1, \dots, M, \quad (7)$$

while the entries of the mixing matrices are

$$\begin{aligned} [\mathbf{W}_d]_{ij} &= \cos \left(\frac{\omega_d}{\Omega_{A/D}} \pi(i-1) \right) \cos \left(\frac{\omega_d}{\Omega_{A/D}} \pi(j-1) \right) \\ &\quad + \sin \left(\frac{\omega_d}{\Omega_{A/D}} \pi(i-1) \right) \sin \left(\frac{\omega_d}{\Omega_{A/D}} \pi(j-1) \right). \end{aligned} \quad (8)$$

Additionally, we define the correlation matrix

$$\boldsymbol{\Sigma}_y(\boldsymbol{\theta}) = \frac{\sum_{d=1}^D \theta_d \frac{\Omega_d}{\pi} \boldsymbol{\Sigma}_d \odot \mathbf{W}_d + \theta_0 \frac{\Omega_0}{\pi} \boldsymbol{\Sigma}_0}{\sum_{d=1}^D \theta_d \frac{\Omega_d}{\pi} + \theta_0 \frac{\Omega_0}{\pi}}. \quad (9)$$

Samples (4) are assumed to follow the Gaussian distribution

$$p_y(\mathbf{y}; \boldsymbol{\theta}) = \frac{\exp \left(-\frac{1}{2} \mathbf{y}^T \mathbf{R}_y^{-1}(\boldsymbol{\theta}) \mathbf{y} \right)}{\sqrt{(2\pi)^M \det(\mathbf{R}_y(\boldsymbol{\theta}))}}. \quad (10)$$

B. Digital data model - Binary sampling

If the signal (1) is digitized via a low-complexity A/D converter with 1-bit amplitude resolution, the measurements are

$$\mathbf{z} = \text{sign}(\mathbf{y}), \quad (11)$$

where the element-wise hard-limiter $\text{sign}(\cdot)$ is defined

$$[\mathbf{z}]_m = \begin{cases} +1 & \text{if } [\mathbf{y}]_m \geq 0, \\ -1 & \text{if } [\mathbf{y}]_m < 0. \end{cases} \quad (12)$$

The output of (11) is invariant to changes of its input scale, such that one can fix $\theta_0 = 1$ and reduce (6) by one element. Like (10), binary distributions are exponential families

$$p_z(\mathbf{z}; \boldsymbol{\theta}) = \exp \left(\mathbf{w}^T(\boldsymbol{\theta}) \boldsymbol{\phi}(\mathbf{z}) - \lambda(\boldsymbol{\theta}) + \nu(\mathbf{z}) \right), \quad (13)$$

where $\mathbf{w}(\boldsymbol{\theta}): \mathbb{R}^D \rightarrow \mathbb{R}^C$ are the statistical weights, $\boldsymbol{\phi}(\mathbf{z}): \mathcal{Z} \rightarrow \mathbb{R}^C$ the sufficient statistics, $\lambda(\boldsymbol{\theta}): \mathbb{R}^D \rightarrow \mathbb{R}$ the log-normalizer, and $\nu(\mathbf{z}): \mathcal{Z} \rightarrow \mathbb{R}$ the carrier measure. In contrast to (10), where $C \in \mathcal{O}(M^2)$, in multivariate binary distributions $C \in \mathcal{O}(2^M)$ as, beside the pairwise products, the sufficient statistics also comprise all higher order products

[17]. Therefore, we use an auxiliary exponential family model [14]

$$\tilde{p}_z(\mathbf{z}; \boldsymbol{\theta}) = \exp \left(\tilde{\mathbf{w}}^T(\boldsymbol{\theta}) \tilde{\boldsymbol{\phi}}(\mathbf{z}) - \tilde{\lambda}(\boldsymbol{\theta}) + \tilde{\nu}(\mathbf{z}) \right), \quad (14)$$

where the sufficient statistics $\tilde{\boldsymbol{\phi}}(\mathbf{z}): \mathcal{Z} \rightarrow \mathbb{R}^{\tilde{C}}$ are

$$\tilde{\boldsymbol{\phi}}(\mathbf{z}) = \boldsymbol{\Phi} \text{vec}(\mathbf{z}\mathbf{z}^T) \quad (15)$$

with $\boldsymbol{\Phi} \in [0; 1]^{\tilde{C} \times M^2}$ being an elimination matrix canceling the duplicate and constant elements of $\mathbf{z}\mathbf{z}^T$. This reduces (13) to a quadratic distribution [18] for which $\tilde{C} \in \mathcal{O}(M^2)$. If

$$\mathbb{E}_{\mathbf{z};\boldsymbol{\theta}} [\tilde{\boldsymbol{\phi}}(\mathbf{z})] = \mathbb{E}_{\tilde{\mathbf{z}};\boldsymbol{\theta}} [\tilde{\boldsymbol{\phi}}(\mathbf{z})], \quad (16)$$

$$\mathbb{E}_{\mathbf{z};\boldsymbol{\theta}} [\tilde{\boldsymbol{\phi}}(\mathbf{z}) \tilde{\boldsymbol{\phi}}^T(\mathbf{z})] = \mathbb{E}_{\tilde{\mathbf{z}};\boldsymbol{\theta}} [\tilde{\boldsymbol{\phi}}(\mathbf{z}) \tilde{\boldsymbol{\phi}}^T(\mathbf{z})], \quad (17)$$

where $\mathbb{E}_{\mathbf{z};\boldsymbol{\theta}}[\cdot]$ denotes the expectation under (13) and $\mathbb{E}_{\tilde{\mathbf{z}};\boldsymbol{\theta}}[\cdot]$ under (14), the Fisher matrices of (13) and (14) satisfy

$$\mathbf{F}_z(\boldsymbol{\theta}) \succeq \tilde{\mathbf{F}}_z(\boldsymbol{\theta}). \quad (18)$$

Without explicit characterization of (13), the information contained in samples from (13) is conservatively quantified by

$$\tilde{\mathbf{F}}_z(\boldsymbol{\theta}) = \left(\frac{\partial \boldsymbol{\mu}_{\tilde{\boldsymbol{\phi}}(\boldsymbol{\theta})}}{\partial \boldsymbol{\theta}} \right)^T \mathbf{R}_{\tilde{\boldsymbol{\phi}}}^{-1}(\boldsymbol{\theta}) \frac{\partial \boldsymbol{\mu}_{\tilde{\boldsymbol{\phi}}(\boldsymbol{\theta})}}{\partial \boldsymbol{\theta}} \quad (19)$$

where

$$\boldsymbol{\mu}_{\tilde{\boldsymbol{\phi}}(\boldsymbol{\theta})} = \mathbb{E}_{\mathbf{z};\boldsymbol{\theta}} [\tilde{\boldsymbol{\phi}}(\mathbf{z})] = \boldsymbol{\Phi} \text{vec}(\mathbf{R}_z(\boldsymbol{\theta})) \quad (20)$$

is obtained by the arcsine law [19]

$$\mathbf{R}_z(\boldsymbol{\theta}) = \frac{2}{\pi} \arcsin(\boldsymbol{\Sigma}_y(\boldsymbol{\theta})). \quad (21)$$

Therefore, the d th column of the derivative of (20) is

$$\left[\frac{\partial \boldsymbol{\mu}_{\tilde{\boldsymbol{\phi}}(\boldsymbol{\theta})}}{\partial \boldsymbol{\theta}} \right]_d = \boldsymbol{\Phi} \text{vec} \left(\frac{\partial \mathbf{R}_z(\boldsymbol{\theta})}{\partial \theta_d} \right) \quad (22)$$

with the off-diagonal matrix entries

$$\left[\frac{\partial \mathbf{R}_z(\boldsymbol{\theta})}{\partial \theta_d} \right]_{ij} = \frac{2}{\pi} \frac{\left[\frac{\partial \boldsymbol{\Sigma}_y(\boldsymbol{\theta})}{\partial \theta_d} \right]_{ij}}{\sqrt{1 - [\boldsymbol{\Sigma}_y(\boldsymbol{\theta})]_{ij}^2}}, \quad \forall i, j : i \neq j, \quad (23)$$

while the diagonal entries are zero. With matrix (9),

$$\frac{\partial \boldsymbol{\Sigma}_y(\boldsymbol{\theta})}{\partial \theta_d} = \frac{\frac{\Omega_d}{\pi} (\boldsymbol{\Sigma}_d \odot \mathbf{W}_d - \boldsymbol{\Sigma}_y(\boldsymbol{\theta}))}{\sum_{d'=1}^D \theta_{d'} \frac{\Omega_{d'}}{\pi} + \frac{\Omega_0}{\pi}}. \quad (24)$$

The covariance matrix of the auxiliary statistics (15)

$$\mathbf{R}_{\tilde{\boldsymbol{\phi}}}(\boldsymbol{\theta}) = \mathbb{E}_{\mathbf{z};\boldsymbol{\theta}} [\tilde{\boldsymbol{\phi}}(\mathbf{z}) \tilde{\boldsymbol{\phi}}^T(\mathbf{z})] - \boldsymbol{\mu}_{\tilde{\boldsymbol{\phi}}(\boldsymbol{\theta})} \boldsymbol{\mu}_{\tilde{\boldsymbol{\phi}}(\boldsymbol{\theta})}^T \quad (25)$$

is obtained by evaluating expectations $\mathbb{E}_{\mathbf{z};\boldsymbol{\theta}} [z_i z_j z_k z_l]$ which, besides (21), requires quadrivariate orthant probabilities [20].

III. PROCESSING TASK

Given $N \in \mathbb{N}$ independent samples of the binary output (11)

$$\mathbf{Z} = [z_1 \quad z_2 \quad \dots \quad z_N], \quad (26)$$

the optimum technique is the MLE. As the binary likelihood (13) is intractable, parameter estimation is here performed by

$$\hat{\boldsymbol{\theta}}(\mathbf{Z}) = \arg \max_{\boldsymbol{\theta} \in \Theta} \sum_{n=1}^N \ln \tilde{p}_z(z_n; \boldsymbol{\theta}). \quad (27)$$

The solution of (27) consistently achieves [14]

$$\begin{aligned} \mathbf{R}_{\hat{\boldsymbol{\theta}}}(\boldsymbol{\theta}) &= \mathbb{E}_{\mathbf{Z}; \boldsymbol{\theta}} \left[(\hat{\boldsymbol{\theta}}(\mathbf{Z}) - \boldsymbol{\theta}) (\hat{\boldsymbol{\theta}}(\mathbf{Z}) - \boldsymbol{\theta})^T \right] \\ &\stackrel{a}{=} \frac{1}{N} \tilde{\mathbf{F}}_z^{-1}(\boldsymbol{\theta}) \end{aligned} \quad (28)$$

and, after computing the empirical mean statistics

$$\hat{\boldsymbol{\mu}}_{\tilde{\boldsymbol{\phi}}}(\mathbf{Z}) = \frac{1}{N} \sum_{n=1}^N \tilde{\boldsymbol{\phi}}(z_n), \quad (29)$$

can be found quickly by $I \in \mathbb{N}$ iterations of scoring [21]

$$\hat{\boldsymbol{\theta}}^{(i)} = \hat{\boldsymbol{\theta}}^{(i-1)} + \Delta \hat{\boldsymbol{\theta}}(\mathbf{Z}; \hat{\boldsymbol{\theta}}^{(i-1)}) \quad (30)$$

with the update term [22]

$$\begin{aligned} \Delta \hat{\boldsymbol{\theta}}(\mathbf{Z}; \boldsymbol{\theta}) &= \left(\left(\frac{\partial \boldsymbol{\mu}_{\tilde{\boldsymbol{\phi}}(\boldsymbol{\theta})}}{\partial \boldsymbol{\theta}} \right)^T \mathbf{R}_{\tilde{\boldsymbol{\phi}}}^{-1}(\boldsymbol{\theta}) \frac{\partial \boldsymbol{\mu}_{\tilde{\boldsymbol{\phi}}(\boldsymbol{\theta})}}{\partial \boldsymbol{\theta}} \right)^{-1} \\ &\quad \cdot \left(\frac{\partial \boldsymbol{\mu}_{\tilde{\boldsymbol{\phi}}(\boldsymbol{\theta})}}{\partial \boldsymbol{\theta}} \right)^T \mathbf{R}_{\tilde{\boldsymbol{\phi}}}^{-1}(\boldsymbol{\theta}) (\hat{\boldsymbol{\mu}}_{\tilde{\boldsymbol{\phi}}}(\mathbf{Z}) - \boldsymbol{\mu}_{\tilde{\boldsymbol{\phi}}(\boldsymbol{\theta})}). \end{aligned} \quad (31)$$

After each update (30), element-wise back-projection $\hat{\boldsymbol{\theta}}^{(i)} = \max(\theta_{\Delta}, \hat{\boldsymbol{\theta}}^{(i)})$ with $\theta_{\Delta} > 0$ ensures that $\hat{\boldsymbol{\theta}}^{(i)} \in \Theta$.

IV. RESULTS

For performance analysis, we define the relative measure

$$\chi_d = \frac{[\mathbf{F}_y^{-1}(\boldsymbol{\theta})]_{dd}}{[\tilde{\mathbf{F}}_z^{-1}(\boldsymbol{\theta})]_{dd}}, \quad (32)$$

where $\mathbf{F}_y(\boldsymbol{\theta})$ denotes the Fisher information matrix of the unquantized samples (4). For verification by Monte-Carlo simulations with the iterative approach (30), we define

$$\hat{\sigma}_d = \frac{1}{\theta_d} \left[\hat{\mathbf{R}}_{\hat{\boldsymbol{\theta}}}^{\frac{1}{2}}(\boldsymbol{\theta}) \right]_{dd} \quad (33)$$

with the empirical error covariance matrix

$$\hat{\mathbf{R}}_{\hat{\boldsymbol{\theta}}}(\boldsymbol{\theta}) = \frac{1}{K} \sum_{k=1}^K (\hat{\boldsymbol{\theta}}(\mathbf{Z}_k) - \boldsymbol{\theta}) (\hat{\boldsymbol{\theta}}(\mathbf{Z}_k) - \boldsymbol{\theta})^T, \quad (34)$$

where K denotes the number of realizations of the data (26).

Two exemplary setups, with $D = 2$, $M = 64$, $N = 10^5$, and $\Omega_{A/D} = \Omega_0$ are considered. In the first scenario, qualitatively depicted in Fig. 1a, sources feature a narrow relative bandwidth $\Omega_d = \frac{\Omega_d}{\Omega_0} = \frac{1}{64}$ while $\bar{\omega}_1 = \frac{\omega_1}{\Omega_0} = \frac{1}{4}$ and $\bar{\omega}_2 = \frac{3}{4}$. Such a situation can occur, for example, in spectrum monitoring of

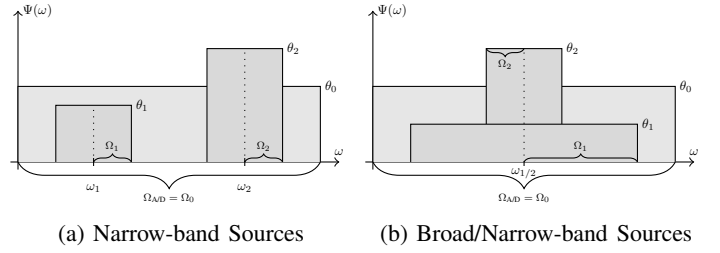


Fig. 1: Example Scenarios

mobile radio frequencies [23]. Fig. 2 visualizes the information loss due to hard-limiting (32) as a function of $\bar{\theta}_2 = \frac{\theta_2}{\theta_0}$ while $\bar{\theta}_1$ is fixed. It can be observed that the loss χ_1 decreases when switching from $\bar{\theta}_1 = -15$ dB to $\bar{\theta}_1 = -3$ dB. The loss χ_2 stays the same in both situations and obtains its minimum around $\bar{\theta}_2 = 12.6$ dB. The plot shows that a large signal-to-noise ratio (SNR) imbalance is unfavorable for the weaker source while the loss can be below $\chi_d = -2$ dB. Fig. 3

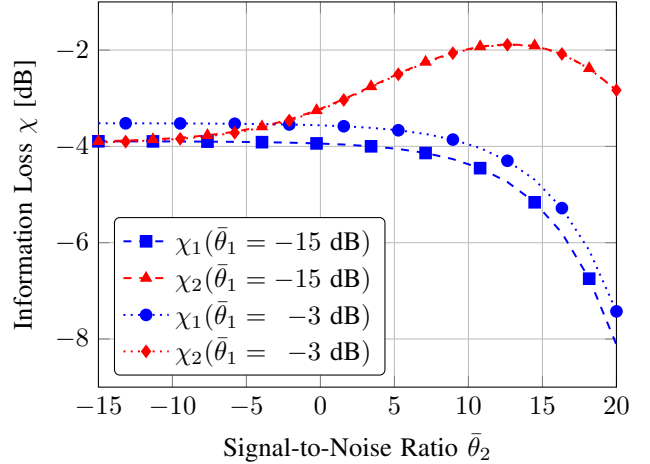


Fig. 2: Information Loss (Narrow Sources)

shows (33) under $\bar{\theta}_1 = -12$ dB when scoring (30) with $I = 5$, $\hat{\boldsymbol{\theta}}^{(0)} = \theta_{\Delta} = -30$ dB, and $K = 10^3$. The empirical results match the analytical results obtained from the inverse Fisher information matrices (dashed and dotted lines).

As a second example, we consider a situation with one broad-band signal source featuring relative bandwidth $\bar{\Omega}_1 = \frac{1}{4}$ and one narrow-band interfering source with $\bar{\Omega}_2 = \frac{1}{64}$ as qualitatively visualized in Fig. 1b. Both sources exhibit $\bar{\omega}_d = \frac{1}{2}$. Such a configuration can be found, for example, in radio astronomical imaging, where the power of weak broad-band electromagnetic emission from a celestial object is measured while terrestrial radio interference occurs in the observed frequency band [24]. Fig. 4 visualizes the hard-limiting loss where the SNR $\bar{\theta}_2$ varies while the SNR $\bar{\theta}_1$ is fixed. Results show that the information loss χ_1 increases when changing from $\bar{\theta}_1 = -15$ dB to $\bar{\theta}_1 = -3$ dB. In contrast, χ_2 slightly decreases for low SNR $\bar{\theta}_2$ while obtaining its minimum around an SNR of $\bar{\theta}_2 = 12$ dB. As for the first scenario with two narrow signal sources, results indicate that SNR imbalance is unfavorable for the weak broad-band source, while the hard-

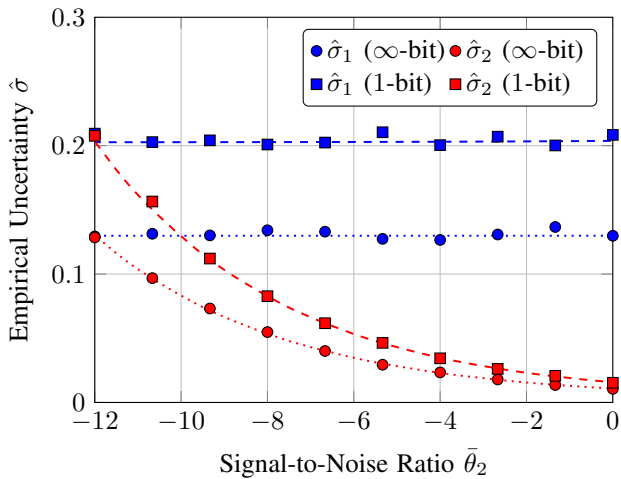


Fig. 3: Uncertainty (Narrow Sources; $\bar{\theta}_1 = -12$ dB)

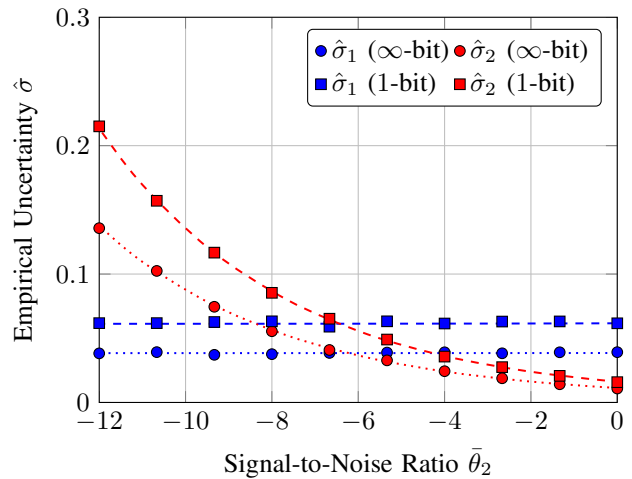


Fig. 5: Uncertainty (Broad/Narrow Sources; $\bar{\theta}_1 = -12$ dB)

limiting loss caused by high SNR interference with narrow bandwidth is less pronounced. Fig. 5 depicts the empirical

achievable sensitivity of likelihood-oriented spectral parameter estimation, i.e., studying cases where $\Omega_{A/D} > \Omega_0$.

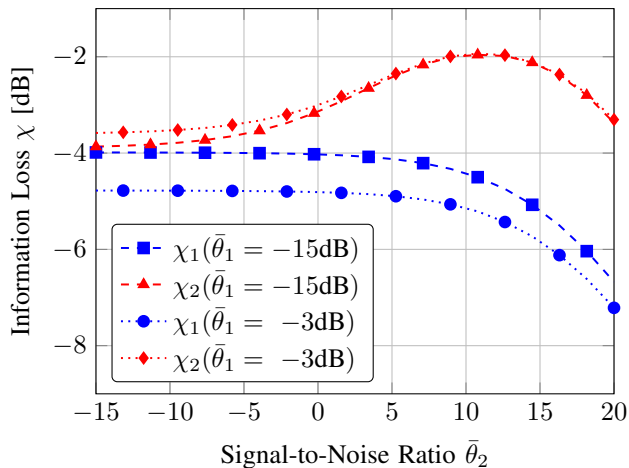


Fig. 4: Information Loss (Broad/Narrow Sources)

results for Monte-Carlo simulations of the Fisher scoring method ($I = 5$, $\hat{\theta}_d^{(0)} = \theta_\Delta = -30$ dB, $K = 10^3$), which are in accordance with the analytical performance analysis.

V. CONCLUSION

We have discussed spectral analysis with binary measurements of random signals under the assumption that the power spectral density structure of the analog sources is known. Using an auxiliary model characterizing multivariate binary distributions, we have obtained the achievable performance and a tractable method for power parameter estimation from the binary samples. The results show that the information loss due to hard-limiting depends on the particular scenario and support that spectral analysis from binary sensor data is, in general, feasible for low to medium SNR configurations when using likelihood-oriented techniques. Future research includes analyzing the potential benefits of oversampling onto the

REFERENCES

- [1] J. H. Van Vleck and D. Middleton, "The spectrum of clipped noise," *Proc. IEEE*, vol. 54, no. 1, pp. 2–19, Jan 1966.
- [2] M. Hinich, "Estimation of spectra after hard clipping of Gaussian processes," *Technometrics*, vol. 9, no. 3, pp. 391–400, 1967.
- [3] S. Weinreb, "A digital spectral analysis technique and its application to radio astronomy," Tech. Rep. 412, Massachusetts Institute of Technology, August 1963.
- [4] B. D. Steinberg, "Hard limiting in synthetic aperture signal processing," *IEEE Trans. Aerosp. Electron. Syst.*, vol. 11, no. 4, pp. 556–561, July 1975.
- [5] A. Ribeiro and G. B. Giannakis, "Bandwidth-constrained distributed estimation for wireless sensor networks - Part I: Gaussian case," *IEEE Trans. Signal Process.*, vol. 54, no. 3, pp. 1131–1143, Mar. 2006.
- [6] A. Mezghani and J. A. Nossek, "On ultra-wideband MIMO systems with 1-bit quantized outputs: Performance analysis and input optimization," in *IEEE Int. Symposium on Information Theory*, June 2007, pp. 1286–1289.
- [7] J. Mo and R. W. Heath, "Capacity analysis of one-bit quantized MIMO systems with transmitter channel state information," *IEEE Trans. Signal Process.*, vol. 63, no. 20, pp. 5498–5512, Oct. 2015.
- [8] C. Mollén, J. Choi, E. G. Larsson, and R. W. Heath, "Uplink performance of wideband massive MIMO with one-bit ADCs," *IEEE Trans. Wireless Commun.*, vol. 16, no. 1, pp. 87–100, Jan. 2017.
- [9] S. Jacobsson, G. Durisi, M. Coldrey, U. Gustavsson, and C. Studer, "Throughput analysis of massive MIMO uplink with low-resolution ADCs," *IEEE Trans. Wireless Commun.*, vol. 16, no. 6, pp. 4038–4051, June 2017.
- [10] S. Rao, A. Mezghani, and A. L. Swindlehurst, "Channel estimation in one-bit massive MIMO systems: Angular versus unstructured models," *IEEE J. Sel. Topics Signal Process.*, vol. 13, no. 5, pp. 1017–1031, Sep. 2019.
- [11] M. S. Stein and M. Fauß, "Latency analysis for sequential detection in low-complexity binary radio systems," to appear in *IEEE Trans. Commun.*, 2019.
- [12] T. J. Schulz, "Penalized maximum-likelihood estimation of covariance matrices with linear structure," *IEEE Trans. Signal Process.*, vol. 45, no. 12, pp. 3027–3038, Dec 1997.
- [13] T. M. Cover and J. A. Thomas, *Elements of Information Theory*, John Wiley & Sons, Ltd, 2005.
- [14] M. S. Stein, J. A. Nossek, and K. Barbé, "Fisher information lower bounds with applications in hardware-aware nonlinear signal processing," *arXiv:1512.03473*, 2015.
- [15] B. Kedem, "Estimation of the parameters in stationary autoregressive processes after hard limiting," *Journal of the American Statistical Association*, vol. 75, no. 369, pp. 146–153, 1980.

- [16] A. Host-Madsen and P. Handel, "Effects of sampling and quantization on single-tone frequency estimation," *IEEE Trans. Signal Process.*, vol. 48, no. 3, pp. 650–662, Mar. 2000.
- [17] B. Dai, S. Ding, and G. Wahba, "Multivariate Bernoulli distribution," *Bernoulli*, vol. 19, no. 4, pp. 1465–1483, 2013.
- [18] D. R. Cox and N. Wermuth, "A note on the quadratic exponential binary distribution," *Biometrika*, vol. 81, no. 2, pp. 403–408, 1994.
- [19] J. B. Thomas, *An introduction to statistical communication theory*, Wiley, 1969.
- [20] M. Sinn and K. Keller, "Covariances of zero crossings in Gaussian processes," *Theory of Probability & Its Applications*, vol. 55, no. 3, pp. 485–504, 2011.
- [21] T. K. Mak, "Solving non-linear estimation equations," *Journal of the Royal Statistical Society. Series B (Methodological)*, vol. 55, no. 4, pp. 945–955, 1993.
- [22] M. S. Stein, "Glancing through massive binary radio lenses: Hardware-aware interferometry with 1-bit sensors," *arXiv:1905.12528*, 2019.
- [23] T. Yucek and H. Arslan, "A survey of spectrum sensing algorithms for cognitive radio applications," *IEEE Commun. Surv. Tutor.*, vol. 11, no. 1, pp. 116–130, 2009.
- [24] P. A. Fridman and W. A. Baan, "RFI mitigation methods in radio astronomy," *Astronomy & Astrophysics*, vol. 378, no. 1, pp. 327–344, 2001.